NeuroMolecular Medicine (2019) 21:85–96
https://doi.org/10.1007/s12017-018-8509-7

ORIGINAL PAPER

Overexpressed TTC3 Protein Tends to be Cleaved into Fragments and Form Aggregates in the Nucleus

Yueqing Gong[1,2,3] · Kun Wang[1,2,3] · Sheng-Ping Xiao[1,2,3] · Panying Mi[1,2,3] · Wanjie Li[2] · Yu Shang[2] · Fei Dou[1,2,3]

Received: 19 April 2018 / Accepted: 31 August 2018 / Published online: 10 September 2018

Abstract

Human *tetratricopeptide repeat domain 3* (*TTC3*) is a gene on 21q22.2 within the Down syndrome critical region (DSCR). Earlier studies suggest that *TTC3* may be an important regulator in individual development, especially in neural development. As an E3 ligase, TTC3 binds to phosphorylated Akt and silence its activity via proteasomal cascade. Several groups also reported the involvement of *TTC3* in familial Alzheimer's disease recently. In addition, our previous work shows that TTC3 also regulates the degradation of DNA polymerase gamma and over-expressed TTC3 protein tends to form insoluble aggregates in cells. In this study, we focus on the solubility and intracellular localization of TTC3 protein. Over-expressed TTC3 tends to form insoluble aggregates over time. The proteasome inhibitor MG132 treatment resulted in more TTC3 aggregates in a short period of time. We fused the fluorescent protein to either terminus of the TTC3 protein and found that the intracellular localization of fluorescent signals are different between the N-terminal tagged and C-terminal tagged proteins. Western blotting revealed that the TTC3 protein is cleaved into fragments of different sizes at multiple sites. The N-terminal sub-fragments of TTC3 are prone to from nuclear aggregates and the TTC3 nuclear import is mediated by signals within the N-terminal 1 to 650 residues. Moreover, over-expressed TTC3 induced a considerable degree of cytotoxicity, and its N-terminal sub-fragments are more potent inhibitors of cell proliferation than full-length protein. Considering the prevalent proteostasis dysregulation in neurodegenerative diseases, these findings may relate to the pathology of such diseases.

Keywords TTC3 · Aggregation · Proteotoxicity · Nuclear localization signal · Alzheimer's disease · Down syndrome

Background

Human *tetratricopeptide repeat* (*TPR*) *domain 3* (*TTC3*) is a gene located on chromosome 21q22.2 within the Down syndrome (DS) critical region (DSCR), and encodes a protein of 2025 amino acid residues (Ohira et al. 1996; Fujiko; Tsukahara et al. 1996). Although a complete extra copy of chromosome 21 is the most common cause of DS, the extra chromosome content can arise in a variety of ways in each case (Antonarakis et al. 2004). In other words, DS phenotypes can be caused by partial trisomy of chromosome 21. According to the latest data, chromosome 21 contains

Yueqing Gong and Kun Wang have contributed equally to this work.

✉ Fei Dou
douf@bnu.edu.cn

Yueqing Gong
goldenlight88@126.com

Kun Wang
201321200091@mail.bnu.edu.cn

Sheng-Ping Xiao
xsp.cau@gmail.com

Panying Mi
mijiapanpan@126.com

Wanjie Li
lwj@bnu.edu.cn

Yu Shang
shangyu@bnu.edu.cn

[1] State Key Laboratory of Cognitive Neuroscience and Learning & IDG/McGovern Institute for Brain Research, College of Life Sciences, Beijing Normal University, Beijing, China

[2] Key Laboratory of Cell Proliferation and Regulation Biology, Ministry of Education, College of Life Sciences, Beijing Normal University, Beijing, China

[3] Center for Collaboration and Innovation in Brain and Learning Sciences, Beijing Normal University, Beijing, China

at least 215 genes (Farrell et al. 2014; Harte et al. 2012; Pruitt et al. 2009). Some of the genes have been studied intensively, such as APP gene, while functions of the others are still not deeply explored. Considering that genes on chromosome 21 contribute to different phenotypes of DS (Antonarakis et al. 2004), the diversity of gene functions and over-expression status leads to phenotypic diversity, which is why DS symptoms vary in patients (Capkova et al. 2014). So further research on the functions of these genes is necessary. DSCR1, which refers to the region covering 21q11.2 and 21q22.1-22.3, is thought to be associated with most DS features (Delabar et al. 1993; Korenberg et al. 1994; Dahmane et al. 1998). As a DSCR1 gene, TTC3 may contribute to certain phenotypes.

Earlier studies have shown that TTC3 expression is regulated in a tissue-specific manner (Ohira et al. 1996; Tsukahara et al. 1996, 1998), and is developmentally regulated during human and mouse embryogenesis (Rachidi et al. 2000; Lopes et al. 1999). TTC3 expression is restricted to the nervous system at later developmental stages (Rachidi et al. 2000; Lopes et al. 1999). Recent years, studies showed that TTC3 affects cell proliferation and differentiation. TTC3 inhibits neuronal differentiation via RhoA and citron kinase (Berto et al. 2007). In addition, as an E3 ligase, TTC3 binds phosphorylated Akt and silence its activity via a proteasomal cascade, leading to a significant accumulation of G2/M cells and inhibiting cell proliferation (Suizu et al. 2009). These results suggest that TTC3 may play an important role in individual development, especially in neural development. Furthermore, TTC3 is reported to be related to Alzheimer disease (AD). It is reported that a rare TTC3 variant was segregated in an extended family with late-onset AD (LOAD), which could contribute to the pathology of the more widespread LOAD (Kohli et al. 2016). It is worth noting that the neuropathology of AD is always present in DS patients aged above 40 (Mann 1988).

Given the potential function of TTC3 in individual development and its relationship to DS and AD, we suspect that TTC3 may be a candidate gene for AD and DS. Aberrant expression of TTC3 can lead to the appearance of the corresponding phenotype. Our previous work shows that TTC3 affects the rate of POLG protein degradation (Gong et al. 2017), which may affect mitochondrial function. In addition, we also found that over-expressed TTC3 tended to form insoluble aggregates in the cells (Gong et al. 2017). In this article, we carry out further exploration. We found that TTC3 aggregates accumulate over time, and MG132 treatment promotes TTC3 aggregation. In addition, we fused the fluorescent protein or Myc-/FLAG-tag to the ends of the TTC3 protein and found that the fluorescent signals of the N-terminal and C-terminal tags are located differently in the cell. The N-terminal fluorescent signal shows aggregates both in the nucleus and in the cytoplasm, whereas the C-terminal signal hardly forms nuclear aggregates. The entry of the N-terminal fragment of TTC3 into the nucleus is mediated by an unidentified NLS, which we consider to be within 1 to 650 amino acid residues of TTC3. In addition, we also obtained similar results with other reports that TTC3 inhibited cell proliferation and found that different fragments produced by hydrolysis of TTC3 have different effects on cell proliferation. Given that many neurodegenerative diseases are characterized by aggregation of proteins, this study may help to discover the potential role of TTC3 in the pathology of neurodegenerative diseases such as DS and AD.

Methods

Cell Culture and Transfection

HEK293T cells were cultured in Dulbecco's Modified Eagle's Medium (DMEM, Thermo Fisher Scientific) supplemented with 10% fetal bovine serum (FBS; Thermo Fisher Scientific) at 37 °C in a humidified incubator with 5% CO_2 (v/v). Neuro2A cells were cultured in DMEM supplemented with 10% FBS and 1% MEM nonessential amino acids (NEAA; Thermo Fisher Scientific) at 37 °C in a humidified incubator with 5% CO_2 (v/v). 293T and N2a cells were transfected by TurboFect Transfection Reagent (Thermo Fisher Scientific).

Plasmid vector containing a partial cDNA fragment of human TTC3 was purchased from Invitrogen. The 1–1478 nt of TTC3 CDS was extended by polymerase chain reaction (PCR) amplification using a pair of primers (TTC3-F1: 5′-CTAGTCGACCATGGACAATTTTGCTGAG; and TTC3-R1: 5′-GCCATCTTGAATTAAGCTTCTCAGC), and the 1479–6078 nt of TTC3 was amplified using another pair (TTC3-F1: 5′-GCGCTGAGAAGCTTAATTCAAGATGGC; and TTC3-R2: 5′-GACGGTACCCTACCTAGAAGAGCAGG).

The full-length TTC3 was subcloned into the pCMV-Myc vector (Clontech), using a pair of primers (forward: 5′-TAATAGTCGACATGGACAATTTTGC-3′; and reverse: 5′-AATACGGTACCCTACCTAGAAGAGC-3′) containing *Sal* I and *Kpn* I restriction sites. Other forms of TTC3 were generated by the restriction digests or PCR amplifications. The nucleotide sequences in the final constructs used in the study were confirmed.

The plasmid mCherry-C1 was a gift from Dr. Zhou Jun, Nankai University, Tianjin.

MG132 Treatment

MG132 is a proteasome inhibitor, and was used to block the ubiquitin–proteasome system in this study.

HEK293T or Neuro2A cells were transfected with indicated vectors. 12 h after transfection, the cells were treated with 10 μM MG132 (Merck Millipore) for another 12 h. MG132 was diluted in dimethylsulfoxide (DMSO; Sigma-Aldrich).

CHX Assay

100 μg/mL cycloheximide (CHX; MP biomedicals) in DMSO was applied to inhibit protein biosynthesis.

293T cells were transfected with indicated plasmids by TurboFect reagents. 12 h after transfection, cells were reseeded into four fresh culture dishes with fresh culture medium. 12 h later, cells were treated with 100 μg/mL of CHX (at time 0). The cells were harvested at indicated time points and lysed with SDS buffer (PBS with 1% SDS) with Roche Protease Inhibitor Cocktail for Western blotting.

Cell Lysis

Cells were lysed in RIPA buffer containing 50 mM Tris–HCl (pH 7.6), 150 mM NaCl, 1% NP-40, 0.1% SDS, 0.5% sodium deoxycholate, and 1× Complete Protease Inhibitor Cocktail (Roche Applied Science). The lysates were clarified by centrifugation at 16,000×*g* for 20 min at 4 °C.

Cells were lysed in SDS buffer (1% SDS/PBS) with Roche Complete Protease Inhibitor Cocktail and sonicated. The lysates were clarified by centrifugation at 16,000×*g* for 20 min at room temperature.

Western Blot Analysis

Cells were extracted with lysis buffer and then mixed with a one-fifth volume of 5× SDS sample buffer (Genstar, E153). 20 μg of the total protein was loaded in each lane of 8% or 10% SDS-PAGE gels. Then the samples were resolved at 70 V (constant voltage). Next, the proteins were transferred to PVDF membranes (Merck Millipore) at 200 mA at 0 °C.

Five hours later, the membranes were blocked in TBST buffer with 5% skimmed milk powder (BD) at room temperature for 1 h. Immunoblotting was carried out with following primary antibodies: mouse monoclonal anti-c-Myc (9E10; Sigma-Aldrich; diluted at 1:5000 in Blocking Buffer), mouse monoclonal anti-FLAG® (M2; Sigma-Aldrich; diluted at 1:5000 in Blocking Buffer), or mouse monoclonal anti-α-tubulin (DM1A; Sigma-Aldrich; diluted at 1:10,000 in Blocking Buffer). The membranes were incubated overnight with antibodies at 4 °C. After three washings with TBST, the membranes were incubated with the secondary antibody (HRP conjugated goat anti-mouse IgG; Sigma-Aldrich; diluted at 1:10,000 in Blocking Buffer). Finally, after three washings with TBST, the membranes were incubated with HRP substrate (Merck Millipore), and the ECL signals were imaged by Clinx ChemiScope 3600 Mini system.

The constituents of the buffers are shown as following:

Running buffer—0.025 M Tris, 0.25 M glycine, 0.1% SDS.
Transfer buffer—0.02 M Tris, 0.15 M glycine, 20% methanol.
TBST buffer—0.075 M Tris, 0.15 M NaCl, 0.05% Tween-20, pH 7.5.
Blocking buffer—TBST buffer with 5% skimmed milk powder.

Indirect Immunofluorescence

Cells which grew on coverslips were fixed with anhydrous methanol for 20 min at − 20 °C. Next, the coverslips were incubated in PBS Buffer with 4% donkey serum for 1 h at room temperature, and then incubated for 1 h with primary antibodies [mouse monoclonal anti-c-Myc (9E10; Sigma-Aldrich), and rabbit monoclonal anti-DYKDDDDK (D6W5B; binds to same epitope as Sigma's Anti-FLAG® M2 Antibody; Cell Signaling)]. After three washings with PBST (PBS with 0.02% TritonX-100), The coverslips were incubated with the secondary antibodies [Donkey anti-Mouse IgG (H + L) Secondary Antibody, Alexa Fluor 488 (ThermoFisher Scientific), and Donkey anti-Rabbit IgG (H + L) Secondary Antibody, Alexa Fluor 546 (ThermoFisher Scientific)] for 1 h at room temperature. Primary and secondary antibodies were diluted at 1:500 in PBS Buffer with 4% donkey serum. Finally, after three washings with PBST, the coverslips were mounted on cover glasses. The cells were imaged by Olympus FV300 confocal microscope.

Live-Cell Imaging

Neuro2A cells were transfected with indicated plasmids by TurboFect reagents. Image recording was performed at indicated time points using the PerkinElmer UltraVIEW VoX 3D Live-Cell Imaging System equipped with an environmental chamber. Cultures were maintained at 37 °C and gassed with 5% CO_2. Images were analyzed with Volocity software.

Proliferation Assays

Proliferation assays were performed and analyzed by IncuCyte® ZOOM Continuous Live-cell Imaging & Analysis System (Essen BioScience). Cells were transfected with indicated vectors. 4 h after transfection, we replaced the old medium with fresh medium. Then the cells were imaged

automatically at indicated time points and analyzed by IncuCyte System. The confluence of the cells was recorded.

Statistical Analysis

Data are shown as mean ± standard error. Statistical significance was determined using the Student's *t* test (two-tailed). Group differences were considered significant at $P < .05$.

Results

TTC3 Protein Forms Aggregates in Cells and Increases in Severity Over Time

Our previous studies showed that TTC3 tended to form insoluble aggregates (Gong et al. 2017). Further research found that aggregation gradually increased over time. N-terminal Venus-TTC3 (Venus-TTC3) was expressed in N2a cells, and confocal microscopy showed that more and more cells formed TTC3 aggregates (Fig. 1a, b). Western blot shows consistent results. Proteins with different solubilities were isolated using a sequential protein extraction method (Fig. 1c). Harvested cells were lysed with RIPA buffer. After centrifugation, RIPA-insoluble pellets were sonicated and dissolved in a buffer containing 1% SDS. We found that TTC3 is present in the RIPA-insoluble portion of the cell and that the amount of insoluble TTC3 increases over time (Fig. 1d, e). It is worth noting that in the WB results we found that insoluble TTC3 protein is hydrolyzed into fragments of different sizes. In the RIPA-insoluble proteolytic fragment of TTC3, the major band has a molecular weight of approximately 130 kDa (as shown in Fig. 1d and the band is marked with an asterisk). In addition, in the range of 35–100 kDa there are four more obvious bands (shown in Fig. 1e, marked with asterisks).

When we treated the cells with the proteasome inhibitor MG132 to block the ubiquitin–proteasome pathway to inhibit protein degradation, we observed more TTC3 aggregates in a short period of time (Fig. 1f, g).

The N- & C-Terminal Fluorescent Signals of Full-Length TTC3 Differ in Intracellular Localization

When we investigated the accumulation of TTC3 in cells, we found an interesting phenomenon. When we transfected N2a cells with TTC3 fused with N-terminal or C-terminal Venus, respectively (Fig. 2a), we found that there were significant differences in intracellular localization between Venus-TTC3 and TTC3-Venus (Fig. 2b). Venus-TTC3 exhibited aggregates in both the nucleus and the cytoplasm, while TTC3-Venus primarily localized in the cytoplasm with less signals in the nucleus,and the aggregates always appeared in the cytoplasm.

Next, N-terminal mCherry-fused TTC3 (mCherry-TTC3, shown in Fig. 2a) and TTC3-Venus were co-transfected into N2a cells for further observation (Fig. 2c). We could also see distinct differences in localization. To explore the cause of the discrepancy in localization, we constructed a vector expressing full-length TTC3 fused with N-terminal Myc-tag and C-terminal 3X FLAG-tag simultaneously (Fig. 2d). N2a cells were transfected with the vector and immunofluorescence staining was performed. For full-length TTC3, the fluorescent signals of the N-terminal and C-terminal tags show distinguishable difference in localization (Fig. 2e), in consistence with the results from the fused fluorescent protein (shown in Fig. 2b, c). The transfected cells were collected and analyzed by Western blots. We found that full-length TTC3 proteins were hydrolyzed into fragments with different molecular weights, and the bands in anti-Myc blots differed from the bands in anti-FLAG blots. (Fig. 2f, left and middle panels). This result indicates that TTC3 can be hydrolyzed at multiple sites. Different proteolytic fragments differ significantly in terms of solubility and intracellular localization.

N-Terminal Sub-fragments of TTC3 Tends to Form Nuclear Aggregates, and TTC3 Nuclear Import is Mediated by a Signal Within the N-Terminal 1–650 Residues

The N-terminal fluorescence signal of TTC3 tended to show nuclear aggregates as described above (Fig. 2b, c, e). We tried to find out the mechanism underneath the entry of TTC3 N-terminal into the nucleus. mCherry-labeled Lamin B2 was co-transfected for labeling the core layer (Fig. 3a).

We found that the nuclear lamina remains intact with nuclear aggregation, indicating that the N-terminal of TTC3 accumulates after entering the nucleus. Next, we used NucPred (Brameier et al. 2007) and cNLS Mapper (Kosugi et al. 2009) for NLS prediction, and the high-score results indicate that there is a potential classical NLS (pNLS, for short) in the region of 1177 to 1185 residues. To verify this predicted NLS, we constructed a vector expressing the N-terminal Venus-fused TTC3 mutant with deletion of this region (Venus-TTC3ΔpNLS), and transfected the vector and wild-type TTC3 into N2a cells. Then we counted the cells with nuclear aggregate formation. However, compared with wild-type TTC3, deletion of the potential NLS did not reduced the number of cells with nuclear spots. No significant difference existed between the two groups (Fig. 3c, d). The predicted NLS did not work in this situation.

So we expanded the search scope. A series of vectors were constructed expressing N-terminal Venus-fused sub-fragments of TTC3. We found that the TTC3 1–650 aa fragment

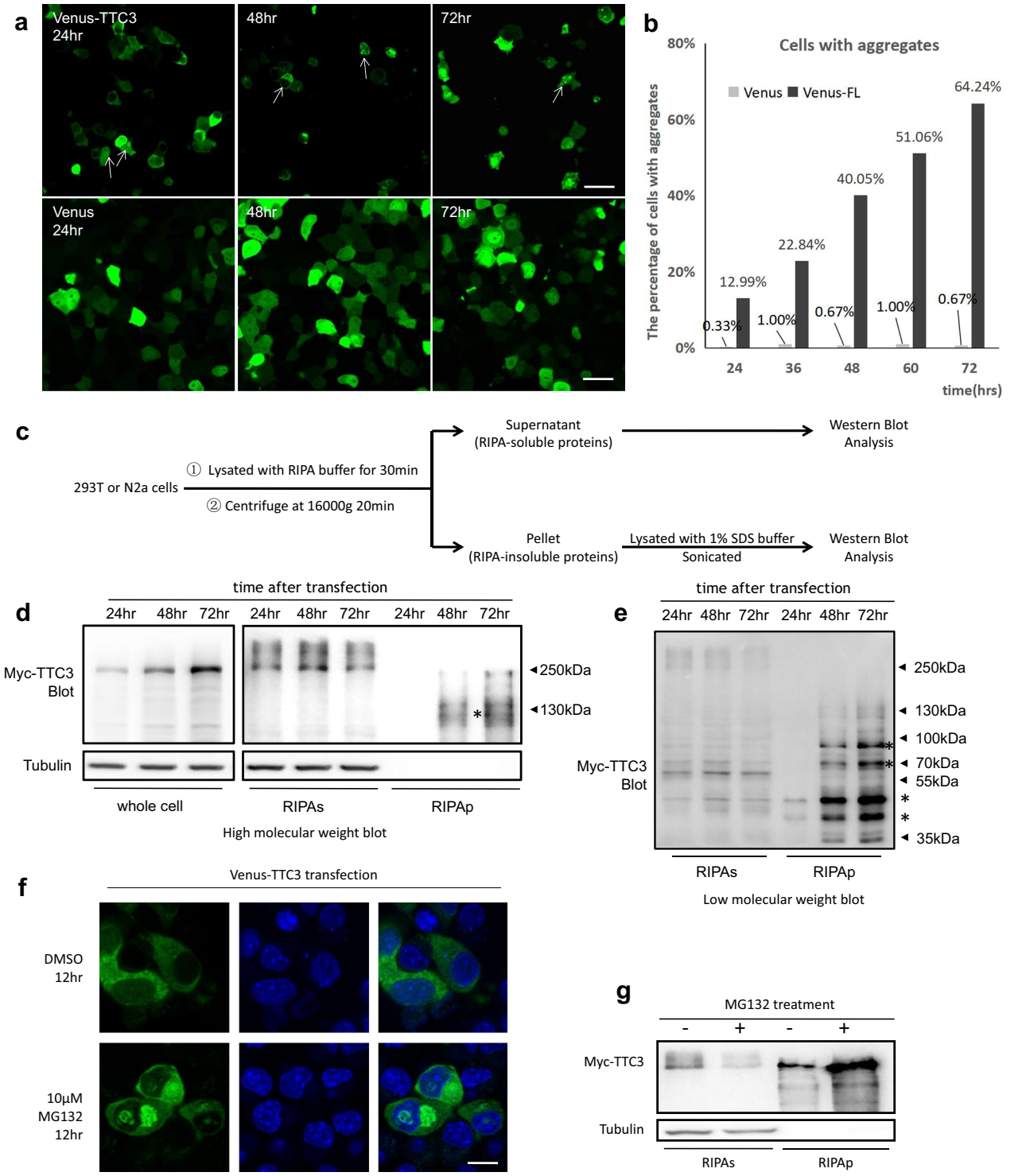

Fig. 1 TTC3 aggregates accumulate over time, and the aggregation process is promoted by MG132 treatment. **a, b** N-terminal Venus-fused TTC3 was expressed in N2a cells. After transfection, the cells were imaged at indicated time point. Three hundred cells were randomly chosen and the ones with aggregates were counted. Confocal microscopy showed that an increasing number of cells formed TTC3 aggregates. The experiments were repeated three times. **c** The process of our sequential protein extraction method. The harvested cells were lysed with RIPA buffer and then centrifuged to isolate the soluble and the insoluble components. **d, e** Western blot analysis of the RIPA-soluble and the RIPA-insoluble fractions of the cells. HEK293T cells were transfected with Myc-TTC3 and then harvested at indicated time point. The insoluble TTC3 increased as time went on. **e** We shortened the time costs of transmembance for the low-molecular-weight proteolytic fragments of TTC3. **f, g** MG132 treatment. **f** N2a cells were transfected with Venus-TTC3, and treated with 10 μM MG132 or an equal volume of DMSO. MG132 promoted aggregate formation. **g** HEK293T cells were transfected with Myc-TTC3, and treated with 10 μM MG132 or an equal volume of DMSO for 12 h. Much more TTC3 proteins presented in the pellets with MG132 treatment

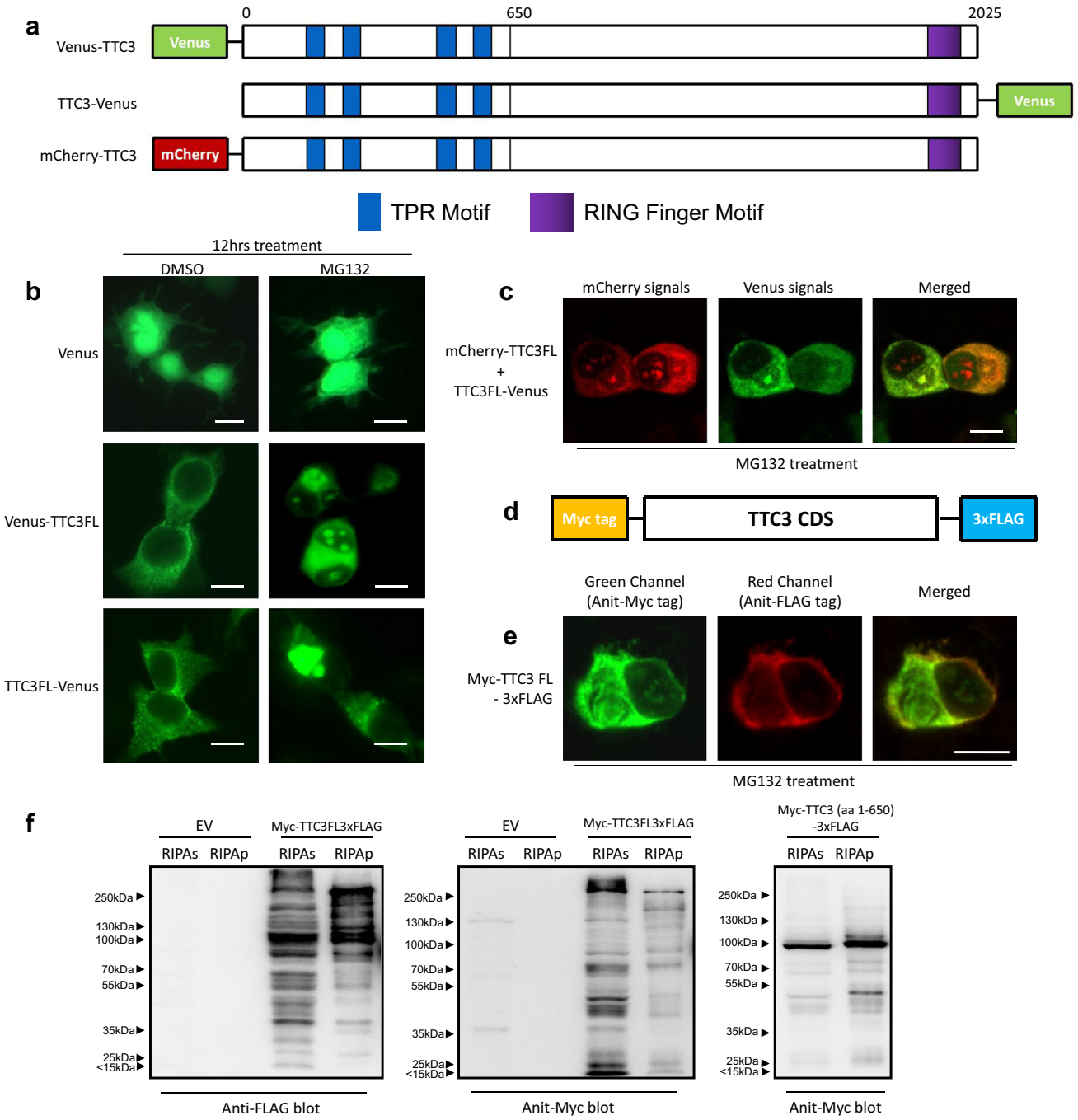

Fig. 2 The N-terminal and C-terminal fluorescent signals of TTC3 differ in intracellular localization. **a** Diagram shows the structure of TTC3 expression vectors used in our study. TTC3 protein was fused with Venus or mCherry. **b** Venus-TTC3 or TTC3-Venus was transfected into N2a cells, and treated with 10 μM MG132 or an equal volume of DMSO. **c** mCherry-TTC3 and TTC3-Venus were co-transfected into N2a cell, and treated with 10 μM MG132 for 12 h. **d** Myc-TTC3FL-3X FLAG. Full-length TTC3 was fused with N-terminal Myc-tag and C-terminal 3X FLAG-tag simultaneously. **e** N2a cells were transfected with Myc-TTC3FL-3X FLAG, and treated with 10 μM MG132 for 12 h. Then we performed indirect immunofluorescence. **f** Western blot analysis. N2a cells were transfected with Myc-TTC3FL-3X FLAG or Myc-TTC3 (aa 1-650)-3X FLAG. 48 h after transfection, the cells were harvested

and other N-terminal sub-fragments with higher molecular weights all exhibited nuclear aggregation (Fig. 3b). We speculate that there is a NLS within the 1–650 residues. So we deleted the N-terminal 1–650 residue (TTC3Δ650), and transfected this N-terminal Venus-fused sub-fragments into cells. We found that Venus-TTC3Δ650 hardly formed nuclear spots with MG132 treatments (Fig. 3e, f). These results suggest that there is a NLS within the 1–650 residues.

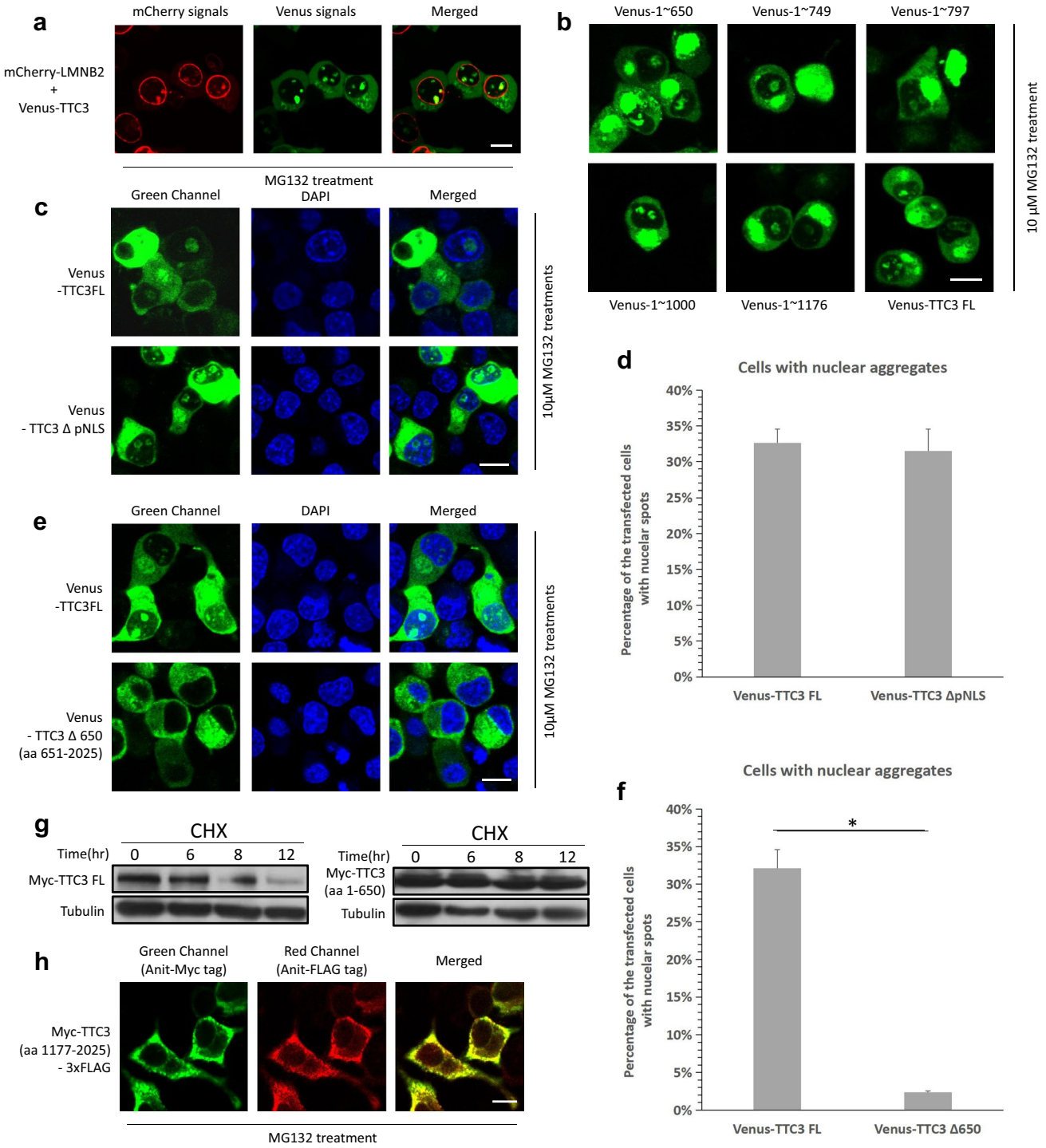

Fig. 3 TTC3 nuclear import is mediated by a signal within the N-terminal 1–650 residues. **a** mCherry-labeled Lamin B2 was utilized to label the nuclear lamina. N2a cells were co-transfected with mCherry-LMNB2 and Venus-TTC3. We found that the nuclear lamina could remain intact with nuclear aggregation. **b** We constructed several vectors to expression the sub-fragments of TTC3, including Venus-TTC3 (aa 1-650), Venus-TTC3 (aa 1-749), Venus-TTC3 (aa 1-797), Venus-TTC3 (aa 1-1000), Venus-TTC3 (aa 1-1176). N2a cells were transfected, and treated with MG132. All the sub-fragments exhibited nuclear spots. **c, d** Venus-TTC3ΔpNLS or Venus-TTC3 was transfected into N2a cells, and treated with MG132. Deletion of the predicted NLS did not reduced the number of cells with nuclear spots. The error bars represent mean ± standard error (SE) ($n = 3$). **e, f** Venus-TTC3Δ650 or Venus-TTC3 was transfected into N2a cells, and treated with MG132. With the deletion of the N-terminal 1–650 residue, TTC3 hardly formed nuclear aggregates. The error bars represent mean ± standard error (SE) ($n = 3$). *$P < .05$. **g** CHX assay. TTC3 1–650 aa has a longer half-life than full-length TTC3. **h** N2a cells were transfected with Myc-TTC3 (aa 1177–2025)-3X FLAG, and treated with MG132. The signals of the N-terminal Myc-tag and C-terminal 3X FLAG-tag were both primarily localized in the cytoplasma

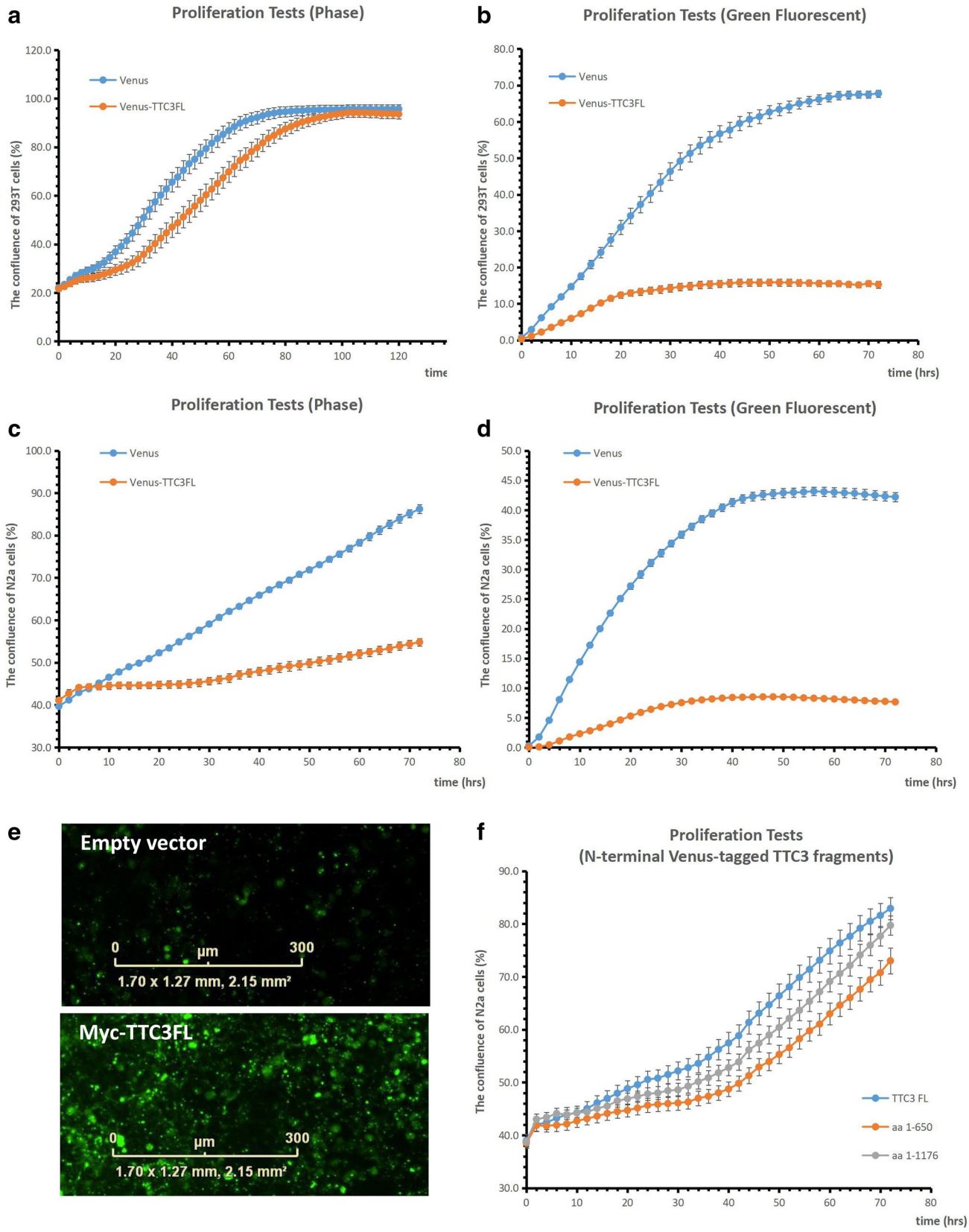
a
Proliferation Tests (Phase)
Venus
Venus-TTC3FL
The confluence of 293T cells (%)
time
b
Proliferation Tests (Green Fluorescent)
Venus
Venus-TTC3FL
The confluence of 293T cells (%)
time (hrs)
c
Proliferation Tests (Phase)
Venus
Venus-TTC3FL
The confluence of N2a cells (%)
time (hrs)
d
Proliferation Tests (Green Fluorescent)
Venus
Venus-TTC3FL
The confluence of N2a cells (%)
time (hrs)
e
Empty vector
0
μm
300
1.70 x 1.27 mm, 2.15 mm²
Myc-TTC3FL
0
μm
300
1.70 x 1.27 mm, 2.15 mm²
f
Proliferation Tests
(N-terminal Venus-tagged TTC3 fragments)
The confluence of N2a cells (%)
TTC3 FL
aa 1-650
aa 1-1176
time (hrs)

◂**Fig. 4** The sub-fragments of TTC3 have discrepant effects on cell proliferation. **a–d** HEK293T (**a, b**) or N2a (**c, d**) cells were transfected with Venus-TTC3 or Venus (control). The total confluence (**a, c**) and the confluence of the fluorescent cells (**b, d**) were recorded by IncuCyte System. **e** The cytotoxicity of TTC3 was evaluated with YOYO-1 (ThermoFisher), a cell-impermeant dsDNA stain. HEK293T cells were transfected with Myc-TTC3 or pCMV-Myc empty vector (control). Then the cells were cultured in the medium with 100 nM YOYO-1. The cells were imaged 48 h after transfection. **f** N2a cells were transfected with Venus-TTC3, Venus-TTC3 (aa 1-650) or Venus-TTC3 (aa 1-1176). The total confluence were recorded by IncuCyte System

In fact, we also found that TTC3 1–650 aa fragments are more likely to form aggregates than full-length proteins. Under the same conditions, 1–650 amino acids of TTC3 formed more aggregates in the cytoplasm than full-length TTC3 (Fig. 3b), suggesting that TTC3 1–650 aa peptides can rapidly form aggregates. Consistently, Western blotting revealed that more 1–650 aa peptides were in the RIPA-insoluble fraction of the cells (Fig. 2f, right panel). In addition, CHX assays were performed to investigate protein degradation, and we found that TTC3 1–650 aa has a longer half-life than full-length proteins (Fig. 3g). In contrast with the N-terminal sub-fragments, the C-terminal sub-fragments hardly formed nuclear aggregates. We transfected N2a cells with Myc-TTC3 (aa 1177–2025)-3X FLAG, and found that the signals of Myc- and 3X FLAG-tags always appeared in the cytoplasm (Fig. 3h). In consideration of the differences in localization between N-terminal fragments and C-terminal fragments, we speculate that full-length TTC3 can be hydrolyzed in the cytoplasm, and the N-terminal proteolytic fragments enter the nucleus and form aggregates.

Full-Length TTC3 Significantly Inhibited Cell Proliferation, While Sub-fragments of TTC3 Have an Effect on Cell Proliferation in Various Degrees

Studies had shown that wild-type TTC3 inhibited cell proliferation (Suizu et al. 2009). We got similar results when 293T and N2a cells were transfected with TTC3. The total confluence and the confluence of the green fluorescent cells were recorded and we found that over-expression of Venus-TTC3 significantly inhibited cell proliferation compared with the control vector (Fig. 5a–d). Considering that TTC3 tends to form aggregates, we evaluated cytotoxicity with YOYO-1, a cell-impermeant stain which shows over a thousand-fold increase in its green fluorescence when bound to dsDNA. Compared with the control, the cells expressing TTC3FL showed us much more green fluorescent signals as a result of the damaged membrane integrity, suggesting that TTC3 over-expression could induce proteotoxicity and cell death (Fig. 4e).

We also monitored the proliferation of cells transfected with TTC3 sub-fragments (Fig. 4f). TTC3 aa 1–650 showed us a stronger inhibitory effect on cell proliferation than the full-length TTC3 and TTC3 aa 1–1176.

Discussion

TTC3 has be reported as a candidate gene of DS and AD, but the mechanisms have not been identified. In DS, the impact of aneuploidy is complex. Many researches have indicated that most genes are expressed in proportion to their copy number, and proteins are translated in strong correlation with the abundance of mRNA (Oromendia and Amon 2014; Stingele et al. 2012). In fact, it has been observed that the abundance of TTC3 protein is higher in Hs52.Sk cells which are derived from DS patients (Suizu et al. 2009). As mentioned above, TTC3 may have some potential functions in individual development, and be an important factor in metabolic regulation. In view of this, one possibility is that the over-expressed TTC3 proteins enhance its original biological functions, resulting in abnormal states during embryonic development, or other biological processes.

At the same time, there is also considerable evidence that aneuploidy results in an unbalanced proteome that causes proteotoxic stress (Oromendia and Amon 2014). The protein quality control systems must not only attend to the excess proteins produced from additional chromosomes, but also support all excess subunits of complexes that are not in stoichiometric ratios with their binding partners (Oromendia and Amon 2014). This can lead to the proteostasis dysregulation. Our previous study has shown that over-expressed TTC3 proteins tends to form aggregates, which is relieved by Hsp70 (Gong et al. 2017). These results imply that the folding process of TTC3 protein may need the full participation of the cellular protein quality control machinery. For this reason, we speculate that TTC3 proteins can accumulate along with the decline of proteostasis. During the exhaustion of the cellular protein quality control machinery, TTC3 proteins can form insoluble aggregates, and maybe oligomers as well. It can produce adverse effects in two aspects. On the one hand, TTC3 is not folded correctly, which results in loss of its physiologic function; on the other hand, TTC3 aggregation can induce neurotoxicity and further worsen the proteostasis.

In AD pathology, TTC3 protein may accumulate and form aggregates owing to the proteostasis dysregulation. It is reported that Aβ accumulation inhibits the activities of the proteasome and deubiquitinating enzymes (Lam et al. 2000). Moreover, in AD, the abnormal activation of proteolytic enzymes, such as caspases (Gamblin et al. 2003; Blandini et al. 2006; Hyman 2011) and calpains (Ferreira 2012; Nilsson et al. 1990), plays an important role in neurodegenerative process. It is possible that TTC3 proteins are hydrolyzed into fragments by some abnormally activated proteases, and

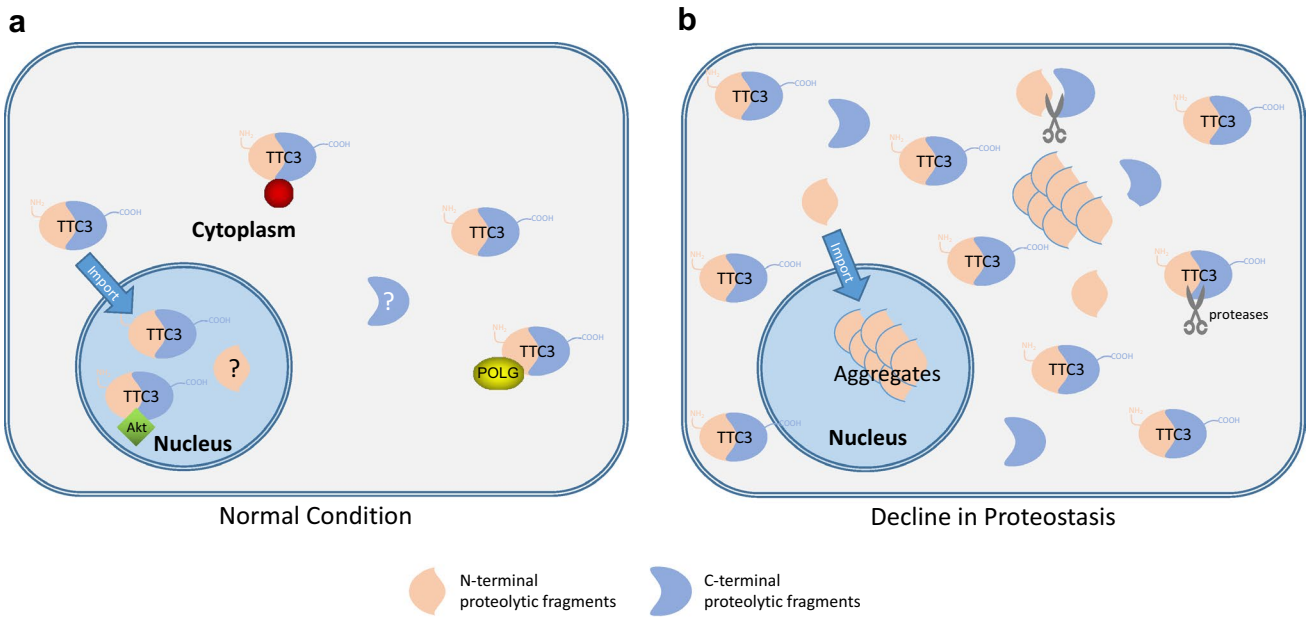

Fig. 5 Dysregulation of proteostasis may lead to the abnormal cleavage and aggregation of TTC3 protein. **a** Normally, TTC3 proteins exist in a nearly full-length form, and its nuclear import is strictly regulated. TTC3 interacts with other molecules, such as Akt and POLG. In this state, TTC3 protein is folded correctly and functional. The shapes marked with "?" indicate that we are not sure if there are also functional proteolytic fragments of TTC3 in normal cells. If they exist, the N-terminal fragments may be localized in the nucleus with the help of the NLS in the region of 1–650 aa. **b** Along with the proteostasis dysregulation, TTC3 proteins accumulate, and are not folded correctly, which results in the exposure of the internal cleavage sites. TTC3 protein is cleaved into fragments by proteolytic enzymes. In neurodegenerative diseases, the activation of certain proteolytic enzymes may also lead to the abnormal cleavage of TTC3. The N-terminal proteolytic fragments can enter the nucleus with the help of the NLS and form aggregates

the characteristics of the proteolytic fragments are diverse, as is shown in this paper.

In our experiments, TTC3 aggregation process is promoted by MG132 treatment, which blocks the ubiquitin–proteasome pathway, disturbing the proteostasis. We also show that the fluorescent signals of N- & C-terminal tags which are linked to TTC3 proteins differ in intracellular localization. These results suggest that the proteolytic fragments of TTC3 protein can vary in localization and solubility, consequently, forming the localization patterns of linked fluorescent signals. In addition, there is a NLS within TTC3 1–650 residues, which can mediate TTC3 N-terminal fragments entering the nucleus. Accordingly, we propose the following model. Under normal circumstances, TTC3 proteins exist in a nearly full-length form, and its nuclear import is strictly regulated (Fig. 5a). However, along with the proteostasis dysregulation, accumulated TTC3 proteins are not folded correctly, and the internal cleavage sites are exposed. As a result, the proteins are hydrolyzed in the cytoplasm. Then the N-terminal proteolytic fragments enter the nucleus with the help of the NLS, and form aggregates (Fig. 5b).

Furthermore, we also monitor the proliferation of cells to evaluate the cytotoxicity induced by TTC3 and its subfragments. Full-length TTC3 inhibits proliferation significantly, and induces a considerable degree of cytotoxicity. The N-terminal fragments showed a stronger inhibitory effect than the C-terminal fragments, which indicates that the cytotoxicity of TTC3 protein is induced predominantly by its N-terminal region. Nevertheless, we have not ruled out the possibility that the soluble N-terminal proteolytic fragments may have some biological functions in the nucleus.

So far, our experiments have been carried out in cultured cells. This is a deficiency of our current work. We do not know if TTC3 protein is hydrolyzed and converted to aggregates in the brain. Next, in vivo experiments should be conducted to assess the cytotoxicity of TTC3 and its tendency to form aggregates, revealing its true role in the pathology of neurodegenerative diseases.

Conclusion

Based on our previous work, we further explore the nature of TTC3 aggregation in cultured cells. First, TTC3 aggregates accumulate over time, facilitating the aggregation process by blocking the ubiquitin–proteasome system. Second, the TTC3 protein can be hydrolyzed into fragments of different sizes by multiple cleavage sites, accompanied by decreased protein homeostasis. Third, the N-terminal fragment of TTC3 tends to form aggregates in the nucleus and its entry

into the nucleus is mediated by signals located within 1–650 residues at the N-terminus. Finally, an excess of TTC3 protein induces cytotoxicity primarily through its N-terminal region. The toxicity of TTC3 may be related to the pathology of neurodegenerative diseases. TTC3 may be a candidate gene for neurodegenerative diseases such as AD and DS.

Acknowledgements The authors will appreciate the support from Experimental Technology Center for Life Sciences, College of Life Sciences, BNU.

Author Contributions FD and YG conceived and designed the study. YG, KW, S-PX and PM performed the experiments. FD and YG wrote the paper. FD, WL and YS reviewed and edited the manuscript. All authors read and approved the manuscript. YG and KW contributed equally to this work.

Funding This work was supported by grants from the National Natural Science Foundation of China (NSFC) (31370768, 30970610) and the Open Research Fund of the State Key Laboratory of Cognitive Neuroscience and Learning.

Compliance with Ethical Standards

Conflict of interest The authors declare that they have no competing interests.

Glossary and Abbreviation

Sub-fragment	The artificially designated fragment which covers a certain region of TTC3 protein and is constructed into expression vectors.
Proteolytic fragment	The proteolytic product of full-length TTC3 or its sub-fragments. Full-length TTC3 and the sub-fragments are cleaved by the intracellular proteases.
N-terminal fragment	The fragment which primarily covers the region near the N-terminus of full-length TTC3 protein.
C-terminal fragment	The fragment which primarily covers the region near the C-terminus of full-length TTC3 protein.
N-terminal tag	The tag peptide which is fused to the N-terminus of full-length TTC3 or its sub fragments.
C-terminal tag	The tag peptide which is fused to the C-terminus of full-length TTC3 or its sub fragments.
N-terminal fluorescent signal	The fluorescent signal which is derived from the N-terminal tag or fluorescent protein fused to the N-terminus of full-length TTC3 or its sub-fragments.
C-terminal fluorescent signal	The fluorescent signal which is derived from the C-terminal tag or fluorescent protein fused to the C-terminus of full-length TTC3 or its sub-fragments.
RIPAs	The RIPA-soluble components of the cells. The cells are lysed with RIPA buffer, and the supernatant is obtained after centrifugation.
RIPAp	The pellets. After centrifugation, the RIPA-insoluble components were made into pellets.

References

Antonarakis, S. E., Lyle, R., Dermitzakis, E. T., Reymond, A., & Deutsch, S. (2004). Chromosome 21 and Down syndrome: From genomics to pathophysiology. *Nature Reviews Genetics, 5*(10), 725–738.

Berto, G., Camera, P., Fusco, C., Imarisio, S., Ambrogio, C., Chiarle, R., et al. (2007). The Down syndrome critical region protein TTC3 inhibits neuronal differentiation via RhoA and Citron kinase. *Journal of Cell Science, 120*(11), 1859–1867.

Blandini, F., Sinforiani, E., Pacchetti, C., Samuele, A., Bazzini, E., Zangaglia, R., et al. (2006). Peripheral proteasome and caspase activity in Parkinson disease and Alzheimer disease. *Neurology, 66*(4), 529–534.

Brameier, M., Krings, A., & Maccallum, R. M. (2007). NucPred—Predicting nuclear localization of proteins. *Bioinformatics, 23*(9), 1159–1160.

Capkova, P., Misovicova, N., & Vrbicka, D. (2014). Partial trisomy and tetrasomy of chromosome 21 without Down Syndrome phenotype and short overview of genotype-phenotype correlation. A case report. *Biomed Pap Med Fac Univ Palacky Olomouc Czech Repub, 158*(2), 321–325.

Dahmane, N., Ghezala, G. A., Gosset, P., Chamoun, Z., Dufresne-Zacharia, M. C., Lopes, C., et al. (1998). Transcriptional map of the 2.5-Mb CBR-ERG region of chromosome 21 involved in Down syndrome. *Genomics, 48*(1), 12–23.

Delabar, J. M., Theophile, D., Rahmani, Z., Chettouh, Z., Blouin, J. L., Prieur, M., et al. (1993). Molecular mapping of twenty-four features of Down syndrome on chromosome 21. *European Journal of Human Genetics, 1*(2), 114.

Farrell, C. M., Leary, N. A. O., Harte, R. A., Loveland, J., Wilming, L., Wallin, C., et al. (2014). Current status and new features of the

Consensus Coding Sequence database. *Nucleic Acids Research, 42*, 865–872.

Ferreira, A. (2012). Calpain dysregulation in Alzheimer's disease. *International Scholarly Research Notices, 2012*, 728571–728571.

Gamblin, T. C., Chen, F., Zambrano, A., Abraha, A., Lagalwar, S., Guillozet, A. L., et al. (2003). Caspase cleavage of tau: Linking amyloid and neurofibrillary tangles in Alzheimer's disease. *Proceedings of the National Academy of Sciences of the United States of America, 100*(17), 10032–10037.

Gong, Y., Wang, X., Shang, X., Xiao, S. P., Li, W., Shang, Y., et al. (2017). Tetratricopeptide repeat domain 3 overexpression tends to form aggregates and inhibit ubiquitination and degradation of DNA polymerase γ. *Oncotarget, 8*(63), 106475–106485.

Harte, R. A., Farrell, C. M., Loveland, J. E., Suner, M.-M., Wilming, L., Aken, B., et al. (2012). Tracking and coordinating an international curation effort for the CCDS Project. *Database: The Journal of Biological Databases and Curation, 2012*, bas008. https://doi.org/10.1093/database/bas008.

Hyman, B. T. (2011). Caspase activation without apoptosis: Insight into Aβ initiation of neurodegeneration. *Nature Neuroscience, 14*(1), 5–6.

Kohli, M. A., Cukier, H. N., Hamiltonnelson, K. L., Rolati, S., Kunkle, B. W., Whitehead, P. L., et al. (2016). Segregation of a rare TTC3 variant in an extended family with late-onset Alzheimer disease. *Neurology Genetics. 2*(1).

Korenberg, J. R., Chen, X. N., Schipper, R., Sun, Z., Gonsky, R., Gerwehr, S., et al. (1994). Down syndrome phenotypes: The consequences of chromosomal imbalance. *Proceedings of the National Academy of Sciences of the United States of America, 91*(11), 4997–5001.

Kosugi, S., Hasebe, M., Tomita, M., & Yanagawa, H. (2009). Systematic identification of cell cycle-dependent yeast nucleocytoplasmic shuttling proteins by prediction of composite motifs. *Proceedings of the National Academy of Sciences of the United States of America, 106*(25), 10171–1017.

Lam, Y. A., Pickart, C. M., Alban, A., Landon, M., Jamieson, C., Ramage, R., et al. (2000). Inhibition of the ubiquitin-proteasome system in Alzheimer's disease. *Proceedings of the National Academy of Sciences of the United States of America, 97*(18), 9902–9906.

Lopes, C., Rachidi, M., Gassanova, S., Sinet, P. M., & Delabar, J. M. (1999). Developmentally regulated expression of mtprd, the murine ortholog of tprd, a gene from the Down syndrome chromosomal region 1. *Mechanisms of Development, 84*(1–2), 189.

Mann, D. M. A. (1988). Alzheimer's disease and Down's syndrome. *Histopathology, 13*(2), 125–137.

Nilsson, E., Alafuzoff, I., Blennow, K., Blomgren, K., Hall, C. M., Janson, I., et al. (1990). Calpain and calpastatin in normal and alzheimer-degenerated human brain tissue. *Neurobiology of Aging, 11*(4), 425–431.

Ohira, M., Ootsuyama, A., Suzuki, E., Ichikawa, H., Seki, N., Nagase, T., et al. (1996). Identification of a novel human gene containing the tetratricopeptide repeat domain from the Down syndrome region of chromosome 21. *DNA Research, 3*(1), 9–16.

Oromendia, A., & Amon, A. (2014). Aneuploidy: Implications for protein homeostasis and disease. *Disease Models & Mechanisms, 7*(1), 15–20.

Pruitt, K. D., Harrow, J., Harte, R. A., Wallin, C., Diekhans, M., Maglott, D., et al. (2009). The consensus coding sequence (CCDS) project: Identifying a common protein-coding gene set for the human and mouse genomes. *Genome Research, 19*(7), 1316–1323.

Rachidi, M., Lopes, C., Gassanova, S., Sinet, P. M., Vekemans, M., Attie, T., et al. (2000). Regional and cellular specificity of the expression of TPRD, the tetratricopeptide Down syndrome gene, during human embryonic development. *Mechanisms of Development, 93*(1), 189–193.

Stingele, S., Stoehr, G., Peplowska, K., Cox, J., Mann, M., & Storchova, Z. (2012). Global analysis of genome, transcriptome and proteome reveals the response to aneuploidy in human cells. *Molecular Systems Biology, 8*(1), 608–608.

Suizu, F., Hiramuki, Y., Okumura, F., Matsuda, M., Okumura, A., Hirata, N., et al. (2009). The E3 ligase TTC3 facilitates ubiquitination and degradation of phosphorylated Akt. *Developmental Cell, 17*(6), 800–810.

Tsukahara, F., Hattori, M., Muraki, T., & Sakaki, Y. (1996). Identification and cloning of a novel cDNA belonging to tetratricopeptide repeat gene family from Down syndrome–critical region 21q22.2. *Journal of Biochemistry, 120*(4), 820–827.

Tsukahara, F., Urakawa, I., Hattori, M., Hirai, M., Ohba, K., Yoshioka, T., et al. (1998). Molecular characterization of the mouse mtprd gene, a homologue of human TPRD: Unique gene expression suggesting its critical role in the pathophysiology of Down syndrome. *Journal of Biochemistry, 123*(6), 1055–1063.